Spacecraft Solar Particle Event (SPE) Shielding: Shielding Effectiveness as a Function of SPE Model as Determined with the FLUKA Radiation Transport Code[1]

Steve Koontz[1], William Atwell[2], Brandon Reddell[1] and Kristina Rojdev[1,3]

[1]NASA Johnson Space Center, Houston, TX 77059 USA

[2]The Boeing Company, Boeing Research & Technology, Houston, TX 77059 USA

[3]PhD Student, University of Southern California, Los Angeles, CA 90024 USA

Poster #: SH51E - 1734

2010 Fall AGU Meeting, SFO, 17 Dec.

INTRODUCTION

Analysis of both satellite and surface neutron monitor data demonstrate that the widely utilized Exponential model of solar particle event (SPE) proton kinetic energy spectra can seriously underestimate SPE proton flux, especially at the highest kinetic energies. The more recently developed Band model produces better agreement with neutron monitor data ground level events (GLEs) and is believed to be considerably more accurate at high kinetic energies. Here, we report the results of modeling and simulation studies in which the radiation transport code FLUKA (FLUKtuierende KAskade) is used to determine the changes in total ionizing dose (TID) and single-event environments (SEE) behind aluminum, polyethylene, carbon, and titanium shielding masses when the assumed form (i. e., Band or Exponential) of the solar particle event (SPE) kinetic energy spectra is changed. FLUKA simulations have fully three dimensions with an isotropic particle flux incident on a concentric spherical shell shielding mass and detector structure. The effects are reported for both energetic primary protons penetrating the shield mass and secondary particle showers caused by energetic primary protons colliding with shielding mass nuclei. Our results, in agreement with previous studies, show that use of the Exponential form of the event spectra can seriously underestimate spacecraft SPE TID and single event environments.

Shielding mass or thickness exterior to each silicon detector shell

Concentric Sphere Shield Thickness (g/cm²)	SiDet1	SiDet1	SiDet1	SiDet1	SiDet1	SiDet1	SiDet1	SiDet1
Polyethylene	0.036	0.175	0.380	1.854	3.677	7.316	18.213	36.719
Carbon	0.074	0.357	0.775	3.783	7.504	14.93	37.169	74.963
Aluminum	0.100	0.482	1.046	5.107	10.131	20.155	50.178	101.164
Titanium	0.167	0.803	1.743	8.512	16.885	33.592	83.603	168.607
Shield Geometric Thickness (cm)	0.056	0.300	0.593	2.926	5.778	11.519	28.704	57.852

The Band integral spectra for the GLEs were computed using the parameters shown on the previous slide and the following expressions:

$$J(>R) = J_0 R^{-\gamma_1}\{[(\gamma_2-\gamma_1)R_0]^{(\gamma_2-\gamma_1)}\exp(\gamma_1-\gamma_2)\}, for\ R \geq (\gamma_2-\gamma_1)R_0.$$

$$J(>R) = J_0\, R^{-\gamma_1}\exp\left(-\frac{R}{R_0}\right), for\ R \leq (\gamma_2-\gamma_1)R_0.$$

For the Exponential spectra, only the J_0 parameter is used

$$J(>R) = J_0 exp\left(-\frac{R}{R_0}\right).$$

Solar particle event Band parameters

Event Start Date	Event Type	J_0(#/cm²)	γ_1	γ_2	R_0(MV)
Nov. 6, 1997	GLE	8.15E+8	0.284	5.38	116
July 14, 2000	GLE	2.94E+9	0.506	7.46	123
July 15, 2000	ESP	6.01E+7	3.235	7.85	226
Nov. 4, 2001	GLE	2.14E+9	0.242	6.67	93
Nov. 4, 2001	ESP	4.78E+8	2.363	11.2	129
Oct. 28, 2003	GLE	8.44E+9	0.0086	6.48	89
Oct. 28, 2003	ESP	1.12E+8	2.812	8.92	171
Oct. 29, 2003	GLE	7.62E+7	2.004	6.86	206

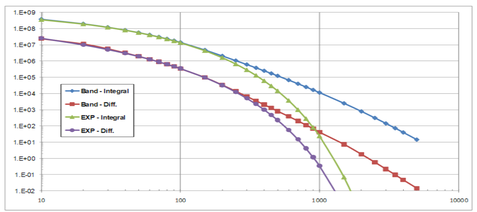

A comparison of the Band & Exponential SPE spectra (integral & differential for the November 1997 SPE.
x-axis: proton energy, MeV; y-axis: integral & diff. fluence, protons/cm² & protons/cm²-MeV.

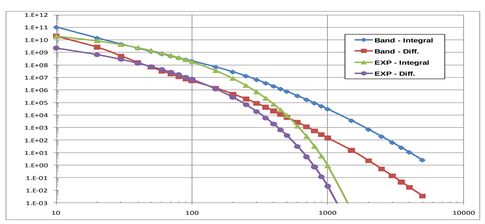

A comparison of the Band & Exponential SPE spectra (integral & differential for the July 2000 SPE.
x-axis: proton energy, MeV; y-axis: integral & diff. fluence, protons/cm² & protons/cm²-MeV.

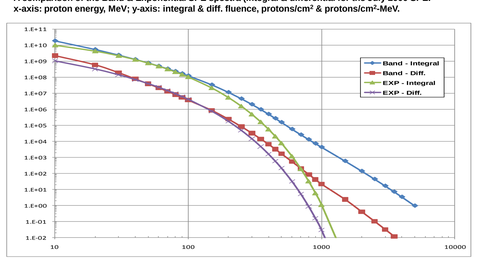

A comparison of the Band & Exponential SPE spectra (integral & differential for the November 2001 SPE.
x-axis: proton energy, MeV; y-axis: integral & diff. fluence, protons/cm² & protons/cm²-MeV.

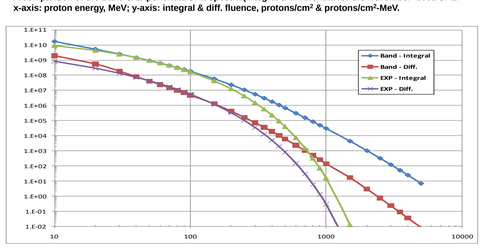

A comparison of the Band & Exponential SPE spectra (integral & differential for the October 2003 SPE.
x-axis: proton energy, MeV; y-axis: integral & diff. fluence, protons/cm² & protons/cm²-MeV.

The plots in this column show the absorbed dose (cGy-Si) as a function of aluminum, polyethylene, carbon and titanium shielding that compare the Band fit with the Exponential fit for the 4 SPEs: July 2000, November 2001, November 1997, and October 2003.

Aluminum

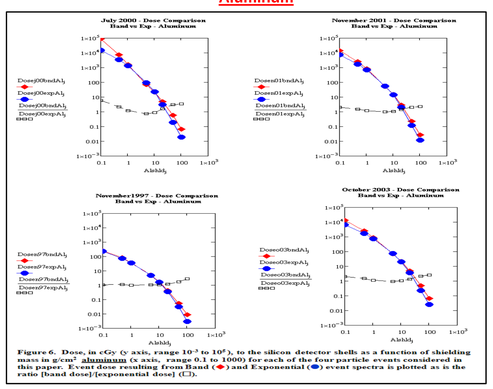

Figure 6. Dose, in cGy (y axis, range 10^{-3} to 10^{4}), to the silicon detector shells as a function of shielding mass in g/cm² aluminum (x axis, range 0.1 to 1000) for each of the four particle events considered in this paper. Event dose resulting from Band (◆) and Exponential (●) event spectra is plotted as is the ratio [band dose]/[exponential dose] (□).

Polyethylene

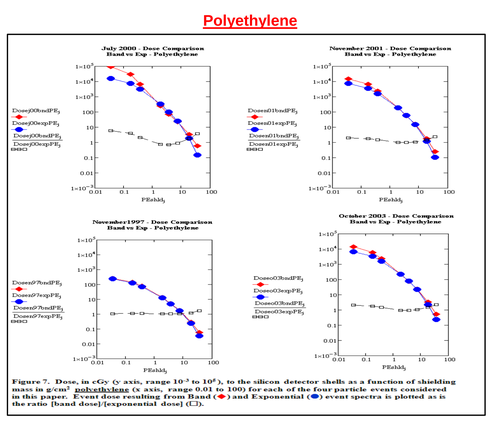

Figure 7. Dose, in cGy (y axis, range 10^{-3} to 10^{4}), to the silicon detector shells as a function of shielding mass in g/cm² polyethylene (x axis, range 0.01 to 100) for each of the four particle events considered in this paper. Event dose resulting from Band (◆) and Exponential (●) event spectra is plotted as is the ratio [band dose]/[exponential dose] (□).

Carbon

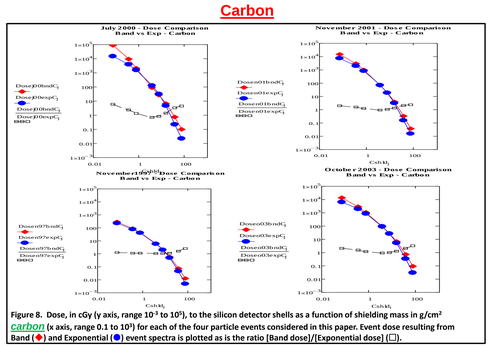

Figure 8. Dose, in cGy (y axis, range 10^{-3} to 10^{5}), to the silicon detector shells as a function of shielding mass in g/cm² carbon (x axis, range 0.1 to 10^{3}) for each of the four particle events considered in this paper. Event dose resulting from Band (◆) and Exponential (●) event spectra is plotted as is the ratio [Band dose]/[Exponential dose] (□).

Titanium

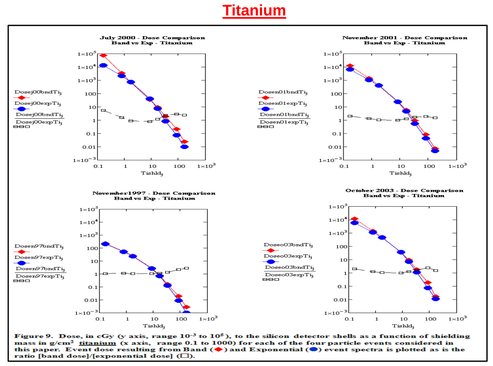

Figure 9. Dose, in cGy (y axis, range 10^{-3} to 10^{5}), to the silicon detector shells as a function of shielding mass in g/cm² titanium (x axis, range 0.1 to 1000) for each of the four particle events considered in this paper. Event dose resulting from Band (◆) and Exponential (●) event spectra is plotted as is the ratio [band dose]/[exponential dose] (□).

The plots in this column show proton star density as a function of aluminum, polyethylene, carbon and titanium shielding that compare the ratio of the Band fit to the Exponential fit for the 4 SPEs: July 2000, November 2001, November 1997, and October 2003.

Aluminum

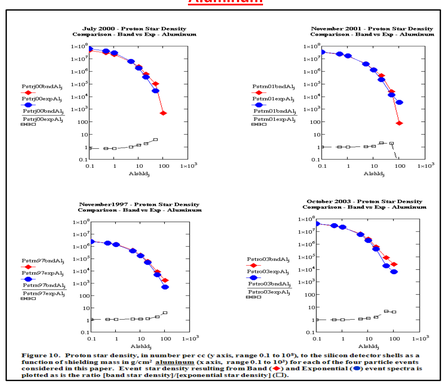

Figure 10. Proton star density, in number per cc (y axis, range 0.1 to 10^{5}), to the silicon detector shells as a function of shielding mass in g/cm² aluminum (x axis, range 0.1 to 10^{3}) for each of the four particle events considered in this paper. Event star density resulting from Band (◆) and Exponential (●) event spectra is plotted as is the ratio [band star density]/[exponential star density] (□).

Polyethylene

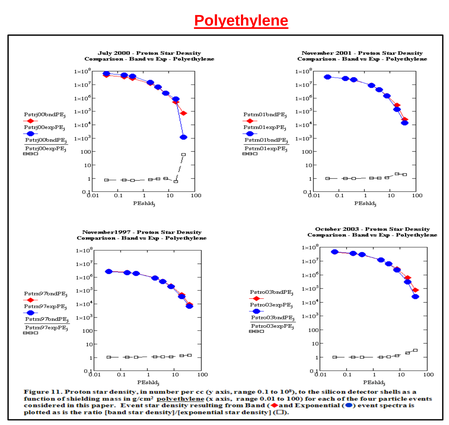

Figure 11. Proton star density, in number per cc (y axis, range 0.1 to 10^{5}), to the silicon detector shells as a function of shielding mass in g/cm² polyethylene (x axis, range 0.01 to 100) for each of the four particle events considered in this paper. Event star density resulting from Band (◆) and Exponential (●) event spectra is plotted as is the ratio [band star density]/[exponential star density] (□).

Carbon

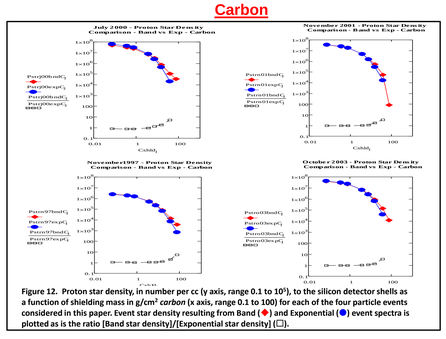

Figure 12. Proton star density, in number per cc (y axis, range 0.1 to 10^{5}), to the silicon detector shells as a function of shielding mass in g/cm² carbon (x axis, range 0.1 to 100) for each of the four particle events considered in this paper. Event star density resulting from Band (◆) and Exponential (●) event spectra is plotted as is the ratio [Band star density]/[Exponential star density] (□).

Titanium

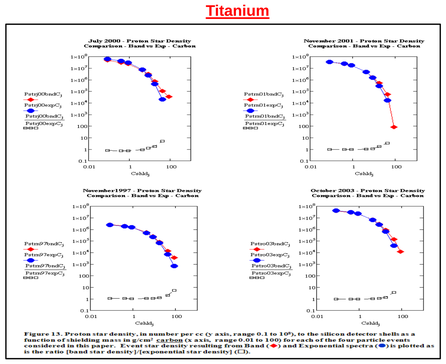

Figure 13. Proton star density, in number per cc (y axis, range 0.1 to 10^{5}), to the silicon detector shells as a function of shielding mass in g/cm² carbon (x axis, range 0.01 to 100) for each of the four particle events considered in this paper. Event star density resulting from Band (◆) and Exponential spectra (●) is plotted as is the ratio [band star density]/[exponential star density] (□).

SUMMARY AND CONCLUSIONS

❖ **The FLUKA radiation transport code has been successfully used to determine changes in the TID environment and the SEE behind aluminum, polyethylene, carbon, and titanium shielding masses when the assumed form (Band or Exponential) of the SPE kinetic energy spectra is changed.**
For all particle event and shielding mass combinations, the following are found to be true: The differences in the TID environment and the SEE between the two SPE spectral forms are most pronounced when the shielding mass is greater than 10 g/cm² or less than 1 g/cm².

❖ **Band and Exponential spectra produce nearly identical results between 1 and 10 g/cm². Direct comparison of SPE spectral forms reveals that the Band form has higher particle fluence than the Exponential form at both low and high kinetic energies, while the two forms are nearly identical at intermediate kinetic energies. It is likely that TID and SEE are dominated by low-energy protons at low (<1g/cm²) shielding mass values and high kinetic energy protons at high (>10g/cm²) shielding mass values while intermediate mass protons dominate dose between 1 and 10 g/cm². Similar results were obtained using the HZETRN deterministic transport code in a simple two-dimensional slab geometry, as shown in the Appendix.**

❖ **The usual atomic number dependence of shielding mass effectiveness was observed. For example, using the Band July 2000 event spectrum, the shielding mass, measured along the sphere radius, needed to reduce the event ionizing dose to 1 cGy or less in the concentric sphere configuration is 30 g/cm² polyethylene, 37 g/cm² carbon, 40 g/cm² aluminum, and 43 g/cm² titanium.**

❖ **Using the Exponential July 2000 event spectrum, the shielding mass needed to reduce the event ionizing dose to 1 cGy or less is 22 g/cm² polyethylene, 25 g/cm² carbon, 29 g/cm² aluminum, and 32 g/cm² titanium.**

❖ **For particle kinetic energies >50 MeV, proton star density displayed a very different dose depth distribution than did neutron and pion star density. Proton star density decreased rapidly with increasing shielding mass and was often overtaken by neutron star density between 10 and 100 g/cm². Pion and neutron star density was nearly constant as shielding mass increased, typically exhibiting a shallow maximum near 10 g/cm².**

❖ **In nearly all cases, the Exponential spectral form produced no pion stars at all – a result expected from the energetic threshold for pion production and the very small number of primary protons above that kinetic energy in the Exponential spectra. The Band and Exponential spectral forms produced comparable secondary neutron yields and plots of star density vs. shielding mass.**

❖ **Calculation of the >50 MeV proton event fluence at various shielding mass values using the corresponding proton star density and the proton inelastic interaction length allowed estimation of SPE SEU counts for three spacecraft that are in reasonable agreement with the observed in-flight SPE SEU counts, thus at least partially confirming the validity of the FLUKA-based modeling process.**

Proton, neutron, and pion star densities as a function of aluminum and polyethylene shielding comparing the Band and Exponential fits for the November 2001 SPE

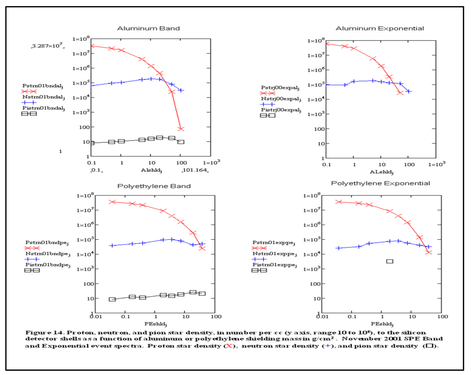

Figure 14. Proton, neutron, and pion star density, in number per cc (y axis, range 10 to 10^{8}), to the silicon detector shells as a function of aluminum or polyethylene shielding matrix g/cm². November 2001 SPE Band and Exponential event spectra. Proton star density (X), neutron star density (+), and pion star density (□).

A comparison of estimated (FLUKA) and observed SPE proton induced single-event rates for three different spacecraft

A comparison of observed in-flight SPE SEU counts with estimates of SPE SEU counts calculated with FLUKA radiation transport code

Spacecraft/System and Device	Nov. 1997 SPE Upsets/bit	July 2000 SPE Upsets/bit	Nov. 2001 SPE Upsets/bit	Oct. 2003 SPE Upsets/bit
Cassini/Solid State Recorder DRAM				
1) Observed upsets	1) 4.4×10^{-7}	NA	NA	NA
2) Estimated upsets	2) 1.4×10^{-7}			
3) Estimated/Observed	3) 0.32			
SOHO /Solid State Recorder DRAM				
1) Observed upsets	1) 4.4×10^{-6}	1) 4.7×10^{-5}	NA	NA
2) Estimated upsets	2) 2.1×10^{-6}	2) 2.1×10^{-5}		
3) Estimated/Observed	3) 0.48	3) 0.4		
Thuraya/ DSP DRAM				
1) Observed upsets	NA	NA	1) 2.0×10^{-6}	1) 1.5×10^{-6}
2) Estimated upsets			2) 2.8×10^{-6}	2) 3.8×10^{-6}
3) Estimated/Observed			3) 1.4	3) 2.5

APPENDIX

Figures a and b below show the results of two-dimensional (slab target) HZETRN dose depth calculations for the Band and Exponential forms of the July 14, 2000 SPE over the shielding mass range 1-100 g/cm². As was observed for the FLUKA 3-D (spherical shell target) calculations, the Band and Exponential spectra produce nearly the same dose over the 1-10 g/cm² shielding mass range while the Band dose exceeds the Exponential dose over the 10-100 g/cm² shielding mass range.
Figures c and d below compare the three-dimensional FLUKA and two-dimensional HZETRN dose-depth results for the July 14, 2000 Band spectra. As expected, the 2-D HZETRN and 3-D FLUKA results are similar at low shielding mass and diverge at higher shielding mass where the 3-D effects of the shielding mass distribution function become more important.

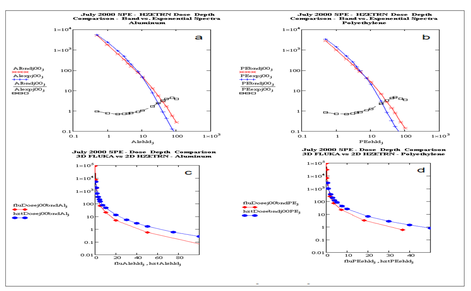

Reference

1) Koontz, S., Atwell, W., Reddell, B., Rojdev, K.; "Spacecraft Solar Particle Event (SPE) Shielding: Shielding Effectiveness as a Functions of SPE Model as Determined with the FLUKA Radiation Transport Code," NASA/TP-2010-216133, September 2010.